16th World Conference on Earthquake Engineering, 16WCEE 2017
Santiago Chile, January 9th to 13th 2017
Paper N° 4485 (Abstract ID)
Registration Code: S-G1464648199

SEISMIC STRUCTURAL HEALTH MONITORING USING BAYESIAN METHODS AND NONLINEAR STRUCTURAL FINITE ELEMENT MODELS

R. Astroza[(1)], H. Ebrahimian[(2)], J.P. Conte[(3)]

[(1)] *Assistant Professor, Facultad de Ingeniería y Ciencias Aplicadas, Universidad de los Andes, Santiago, Chile, rastroza@miuandes.cl*
[(2)] *Postdoctoral Scholar, Department of Mechanical and Civil Engineering, California Institute of Technology, hebrahim@caltech.edu*
[(3)] *Professor, Department of Structural Engineering, University of California, San Diego, jpconte@ucsd.edu*

Abstract

This paper presents an approach for structural health monitoring by integrating nonlinear structural finite element (FE) models and Bayesian methods. Batch and recursive Bayesian estimation methods are used to calibrate/update a nonlinear structural FE model of a structure (e.g., building, bridge, dam, etc.) employing the input-output dynamic data recorded during an earthquake event. Unknown parameters of the nonlinear FE model describing inertia, geometric, material constitutive models, and/or constraint properties of the structure are estimated using spatially-sparse response data recorded by homogeneous or heterogeneous sensor arrays. The updated nonlinear FE model is then used to assess the state of health or damage of the structure. The recursive Bayesian estimation method processes the measured data recursively, and updates the estimation of the FE model parameters progressively over the time history of the event. The recursive Bayesian estimation method results in a nonlinear Kalman filtering approach. The Extended Kalman filter (EKF) and Unscented Kalman filter (UKF) are employed as recursive Bayesian estimation methods. The batch estimation method is based on a maximum a posteriori estimation (MAP) approach, where the time history of the input and output measurements are used as a single batch of data for estimating the FE model parameters. This method results in a nonlinear optimization problem that is solved using a gradient-based optimization algorithm. For those estimation methods requiring the computation of structural FE response sensitivities with respect to the unknown FE model parameters, the direct differentiation method (DDM) is employed. Response data numerically simulated from a nonlinear FE model with unknown material model parameters of a five-story two-by-one bay reinforced concrete frame building subjected to bi-directional horizontal seismic excitation are used to illustrate the performance of the proposed framework.

Keywords: Structural health monitoring; Nonlinear finite element model; Bayesian methods; Damage identification; System identification

1. Introduction

Damage identification (DID) is one of the main goals of structural health monitoring (SHM). The capability of assessing the state of damage (or health) of a structural system and, therefore, of evaluating the risk involved in the post-disaster occupancy (or operation) of the structure is of vital importance. Finite element (FE) model updating, which can be defined as the process of calibrating a FE model to minimize the discrepancy between the measured and FE predicted responses of a structure, is a powerful DID method for structural systems. Linear FE model updating has been one of the most popular approaches for DID of civil structures. In this technique, linear FE models are calibrated using low amplitude vibration data recorded before and after a potentially damaging event and damage is characterized as the reduction of effective stiffness over one or more regions of the structure [1]. Despite its popularity in the field of structural engineering, linear FE model updating cannot provide any information about the inelastic response regime in the structural components and system (e.g., history of plastic deformations, residual deformations, loss of strength, etc.), information that is essential for a comprehensive condition assessment of the structure. In recent years, a number of efforts have been undertaken in the field of nonlinear FE model updating of civil structures [2],[3]. Distefano and co-workers contributed pioneering work in this topic in the 1970's [4],[5]. The studies presented in the literature have utilized simplified nonlinear structural models with lumped nonlinearities defined phenomenologically, through for example the Bouc-Wen plasticity model, to describe the hysteretic force-deformation response behavior of the structure at the story level or at the plastic hinge zones. However, such models are not used for high-fidelity mechanics-based structural FE modeling; because they fall short in accurately simulating the nonlinear response behavior of real-world structures under extreme loading conditions. Recently, the problem of updating mechanics-based nonlinear FE models of structures using input-output data recorded during damage-inducing events has been investigated [6]-[8]. An advanced mechanics-based FE model, updated using the measured input-output data, is able to capture actual damage mechanisms in the structural system and thus can provide accurate information about the presence, location, type, and extent of damage in the structure.

This paper describes the use of batch and recursive Bayesian estimation methods to update mechanics-based nonlinear FE models of civil structures using input-output dynamic data recorded during an earthquake event. The batch method is based on a maximum a posteriori (MAP) approach, resulting in a constrained nonlinear optimization problem that is solved using gradient-based optimization algorithm. The recursive method results in a nonlinear Kalman filtering approach. The Extended Kalman filter (EKF) and Unscented Kalman filter (UKF) are employed as recursive Bayesian estimation methods. Implementation of the EKF and MAP method requires the FE response sensitivities with respect to the model parameters to be estimated. These sensitivities are computed using the direct differentiation method (DDM), an accurate and computationally efficient approach based on the exact (consistent) differentiation of the FE numerical scheme with respect to the model parameters [9]. An application example is presented based on data simulated numerically from a realistic nonlinear FE model of a three-dimensional (3D) five-story two-by-one bay reinforced concrete (RC) frame building subjected to bi-directional horizontal earthquake excitation.

2. Bayesian FE model updating

In this section, different approaches for the identification of nonlinear structural FE models based on the Bayesian method are presented. First, a general Bayesian framework for FE model updating is described. Then, the batch and recursive methods for estimating the unknown FE model parameters and quantifying their uncertainty are introduced.

The time-discretized equation of motion of an n-DOF nonlinear FE model of a structural system at time step i subjected to rigid base earthquake excitation can be written as

$$\mathbf{M}(\boldsymbol{\theta})\ddot{\mathbf{q}}_i(\boldsymbol{\theta}) + \mathbf{C}(\boldsymbol{\theta})\dot{\mathbf{q}}_i(\boldsymbol{\theta}) + \mathbf{r}_i\left(\mathbf{q}_i(\boldsymbol{\theta}), \boldsymbol{\theta}\right) = -\mathbf{M}(\boldsymbol{\theta})\mathbf{L}\ddot{\mathbf{u}}_{g_i} \tag{1}$$

in which $\mathbf{q}_i, \dot{\mathbf{q}}_i, \ddot{\mathbf{q}}_i \in \mathbb{R}^{n\times 1}$ = relative displacement, velocity, and acceleration response vectors, respectively, $\mathbf{M} \in \mathbb{R}^{n\times n}$ = mass matrix, $\mathbf{C} \in \mathbb{R}^{n\times n}$ = damping matrix, $\mathbf{r}_i\left(\mathbf{q}_i(\boldsymbol{\theta}), \boldsymbol{\theta}\right) \in \mathbb{R}^{n\times 1}$ = history-dependent internal

resisting force vector, $\boldsymbol{\theta} \in \mathbb{R}^{n_{\boldsymbol{\theta}} \times 1}$ = FE model parameter vector, $\mathbf{L} \in \mathbb{R}^{n \times n_{\ddot{\mathbf{u}}_g}}$ = influence matrix and $\ddot{\mathbf{u}}_{g_i} \in \mathbb{R}^{n_{\ddot{\mathbf{u}}_g} \times 1}$ = input ground acceleration vector where $n_{\ddot{\mathbf{u}}_g}$ = number of base excitation components. From Eq. (1), the response of the FE model at time step i can be expressed as a nonlinear function mapping the FE model parameters and the input ground acceleration time history to the FE predicted response vector (see [10] for more details), i.e.,

$$\hat{\mathbf{y}}_i = \mathbf{h}_i\left(\boldsymbol{\theta}, \ddot{\mathbf{u}}_{g_{1:i}}\right) \tag{2}$$

where $\hat{\mathbf{y}}_i \in \mathbb{R}^{n_{\mathbf{y}} \times 1}$ = FE predicted response, $\ddot{\mathbf{u}}_{g_{1:i}} = [\ddot{\mathbf{u}}_{g_1}{}^T, \ddot{\mathbf{u}}_{g_2}{}^T, ..., \ddot{\mathbf{u}}_{g_i}{}^T]^T$, and $\mathbf{h}_i(...)$ = nonlinear response function of the FE model. The dynamic response of the structure can be recorded using an array of heterogeneous sensors such as accelerometers, GPS antennas, strain gauges, etc. The measured structural response vector, $\mathbf{y}_i$, can be related to the FE predicted response vector, $\hat{\mathbf{y}}_i$, using the prediction error framework, i.e.,

$$\mathbf{v}_i(\boldsymbol{\theta}) = \mathbf{y}_i - \mathbf{h}_i\left(\boldsymbol{\theta}, \ddot{\mathbf{u}}_{g_{1:i}}\right) \tag{3}$$

where $\mathbf{v}_i$, the simulation error, stands for the discrepancies between the measured and FE predicted responses. It accounts for the measurement noise, errors in the FE model parameters, and analytical model uncertainties. It is ideally assumed that the FE model can capture exactly the real-world physics of the structural response and, therefore, the analytical model uncertainties are neglected. Moreover, it is assumed that the time history of the input ground acceleration is deterministic and known. By neglecting the effects of model uncertainties and assuming that the measurement noise is Gaussian white, the simulation error at each time step can be modeled as a stationary independent zero-mean Gaussian white noise vector process. Therefore, it follows that

$$p(\mathbf{v}_i) = \frac{1}{(2\pi)^{n_{\mathbf{y}}/2} |\mathbf{R}|^{1/2}} e^{-\frac{1}{2}\mathbf{v}_i^T \mathbf{R}^{-1} \mathbf{v}_i} \tag{4}$$

where $|\mathbf{R}|$ denotes the determinant of the diagonal matrix $\mathbf{R} \in \mathbb{R}^{n_{\mathbf{y}} \times n_{\mathbf{y}}}$ defined as the time invariant covariance matrix of the simulation error vector (i.e., $\mathbf{R} = E(\mathbf{v}_i \mathbf{v}_i^T), \forall i$). The unknown FE model parameter vector $\boldsymbol{\theta}$ is modeled as a random vector (denoted by $\boldsymbol{\Theta}$) according to the Bayesian approach for parameter estimation. Bayes' rule is employed to derive the posterior joint probability density function (PDF) of the model parameters from the time histories of the noisy output measurements and the prior joint PDF of these parameters, i.e.,

$$p\left(\boldsymbol{\theta} \middle| \mathbf{y}_{1:k}\right) = \frac{p\left(\mathbf{y}_{1:k} \middle| \boldsymbol{\theta}\right) p(\boldsymbol{\theta})}{p\left(\mathbf{y}_{1:k}\right)} \tag{5}$$

in which $\mathbf{y}_{1:k} = \left[\mathbf{y}_1{}^T, \mathbf{y}_2{}^T, ..., \mathbf{y}_k{}^T\right]^T$ = time history of the measured response of the structure, and $p\left(\mathbf{y}_{1:k} \middle| \boldsymbol{\theta}\right)$ = likelihood function. According to Eq. (3), it follows that

$$p\left(\mathbf{y}_{1:k} \middle| \boldsymbol{\theta}\right) = p\left(\mathbf{v}_{1:k}\right) = \prod_{i=1}^{k} p\left(\mathbf{v}_i\right) \tag{6}$$

The objective of the nonlinear FE model updating framework is to estimate the value of the unknown FE model parameter vector $\boldsymbol{\theta}$ at which the posterior joint PDF of $\boldsymbol{\Theta}$ given the measured structural response is maximum, i.e.,

$$(\hat{\boldsymbol{\theta}})_{\text{MAP}} = \arg\max_{(\boldsymbol{\theta})} p(\boldsymbol{\theta} | \mathbf{y}_{1:k}) \tag{7}$$

where MAP stands for maximum a posteriori estimate. Two different approaches to solve this problem are presented in this paper: (1) batch Bayesian estimation method, and (ii) recursive Bayesian estimation method.

2.1 Batch Bayesian estimation method

The entire time history of the measured data is used as a batch of data to update the posterior PDF of the FE model parameters and find the MAP estimate. Assuming a Gaussian distribution for $p(\boldsymbol{\theta})$ in Eq. (5) and that the response time history is available from the first to the k^{th} time step, it can be shown that

$$\log\left(p\left(\boldsymbol{\theta}|\mathbf{y}_{1:k}\right)\right) = c_0 - \frac{kn_y}{2}\log(2\pi) - \frac{k}{2}\log\left(|\mathbf{R}|\right) - \frac{1}{2}\sum_{i=1}^{k}\left(\mathbf{y}_i - \mathbf{h}_i\left(\boldsymbol{\theta}, \ddot{\mathbf{u}}_{g_{1:i}}\right)\right)^T \mathbf{R}^{-1}\left(\mathbf{y}_i - \mathbf{h}_i\left(\boldsymbol{\theta}, \ddot{\mathbf{u}}_{g_{1:i}}\right)\right) - \frac{n_{\boldsymbol{\theta}}}{2}\log(2\pi) - \frac{1}{2}\log\left(\left|\hat{\mathbf{P}}_0\right|\right) - \frac{1}{2}\left(\boldsymbol{\theta} - \hat{\boldsymbol{\theta}}_0\right)^T \left(\hat{\mathbf{P}}_0\right)^{-1}\left(\boldsymbol{\theta} - \hat{\boldsymbol{\theta}}_0\right) \tag{8}$$

in which $c_0 = -\log(p(\mathbf{y}_{1:k}))$ is a constant, $\hat{\boldsymbol{\theta}}_0$ is the prior mean estimate of $\boldsymbol{\Theta}$, and $\hat{\mathbf{P}}_0$ is the prior covariance matrix of $\boldsymbol{\Theta}$, which quantifies the uncertainties associated with the prior estimates of the FE model parameters.

The diagonal entries of $\mathbf{R}$ (variances of the components of the simulation error vector) can also be treated as random variables and estimated jointly with the FE model parameters through an extended estimation, which allows for automatic information assimilation from the data measured by heterogeneous sensor arrays.

The MAP problem defined in Eq. (7) results in the following minimization problem:

$$\left(\hat{\boldsymbol{\theta}}, \hat{\mathbf{r}}\right)_{\text{MAP}} = \arg\min_{(\boldsymbol{\theta}, \mathbf{r})} J\left(\mathbf{r}, \boldsymbol{\theta}, \mathbf{y}_{1:k}, \ddot{\mathbf{u}}_{g_{1:k}}\right) \tag{9}$$

$$J\left(\mathbf{r}, \boldsymbol{\theta}, \mathbf{y}_{1:k}, \ddot{\mathbf{u}}_{g_{1:k}}\right) = \frac{k}{2}\sum_{j=1}^{n_y}\log\left(r_j\right) + \frac{1}{2}\sum_{i=1}^{k}\left(\mathbf{y}_i - \mathbf{h}_i\left(\boldsymbol{\theta}, \ddot{\mathbf{u}}_{g_{1:i}}\right)\right)^T \mathbf{R}^{-1}\left(\mathbf{y}_i - \mathbf{h}_i\left(\boldsymbol{\theta}, \ddot{\mathbf{u}}_{g_{1:i}}\right)\right) + \frac{1}{2}\left(\boldsymbol{\theta} - \hat{\boldsymbol{\theta}}_0\right)^T \left(\hat{\mathbf{P}}_0\right)^{-1}\left(\boldsymbol{\theta} - \hat{\boldsymbol{\theta}}_0\right) \tag{10}$$

in which $\mathbf{r} \in \mathbb{R}^{n_y \times 1}$ is the vector of the diagonal entries of matrix $\mathbf{R}$. This minimization problem is solved using the interior-point method [11], a gradient-based minimization algorithm. It requires the computation of the gradi0065nt of the objective function with respect to the optimization parameters, which in turn requires the FE response sensitivities with respect to the FE model parameters. The latter can be computed accurately and efficiently utilizing the DDM (e.g., [9],[12]).

The Posterior Cramér–Rao lower bound (PCRLB) theorem [13] can be used to quantify the parameter estimation uncertainties and to estimate a lower bound for the covariance matrix of the estimated FE model parameters. The lower bounds for the estimation problem shown in Eq. (9) can be derived as [10]

$$\text{Cov}\left(\boldsymbol{\Theta}\right) \geq \left(\sum_{i=1}^{k}\left[\left(\frac{\partial \mathbf{h}_i\left(\boldsymbol{\theta}, \ddot{\mathbf{u}}_{g_{1:i}}\right)}{\partial \boldsymbol{\theta}}\right)^T \mathbf{R}^{-1} \frac{\partial \mathbf{h}_i\left(\boldsymbol{\theta}, \ddot{\mathbf{u}}_{g_{1:i}}\right)}{\partial \boldsymbol{\theta}}\right]_{\hat{\boldsymbol{\theta}}, \hat{\mathbf{R}}} + \left(\hat{\mathbf{P}}_0\right)^{-1}\right)^{-1} \tag{11}$$

$$\text{Cov}\left(R_i\right) \geq \frac{k}{2}\frac{1}{\hat{r}_i^2} \tag{12}$$

in which R_i is a random variable characterizing the i^{th} diagonal entry of matrix $\mathbf{R}$. The right-hand side of Eq. (11) is the inverse of the Fisher Information matrix and can be approximated by the Hessian matrix of the objective function J in Eq. (10). Then, two methods can be used to quantify the parameter estimation uncertainty. The first is based on computing the Fisher Information matrix, as shown in Eq. (11), which is referred to as Method 1 in this paper. Referred to as Method 2, the second method is based on the computation of the Hessian matrix of the objective function in Eq. (10). The Hessian matrix is a by-product of the optimization procedure and is approximately estimated using the Broyden-Fletcher-Goldfarb-Shanno (BFGS) method [14].

2.2 Recursive Bayesian estimation method

2.2.1 Extended Kalman filter (EKF)

The MAP problem (Eq. (7)) can also be solved using a recursive (time step by time step) solution approach. The MAP estimate of $\boldsymbol{\Theta}$ at time step *i* is derived by differentiating Eq. (8) with respect to $\boldsymbol{\theta}$ and solving for $\boldsymbol{\theta}$, i.e.,

$$\frac{\partial \log\left(p\left(\boldsymbol{\theta}|\mathbf{y}_i\right)\right)}{\partial \boldsymbol{\theta}} = 0 \;\Rightarrow\; \left(\mathbf{y}_i - \mathbf{h}_i\left(\boldsymbol{\theta}, \ddot{\mathbf{u}}_{g_{1:i}}\right)\right)^T \mathbf{R}^{-1} \frac{\partial \mathbf{h}_i\left(\boldsymbol{\theta}, \ddot{\mathbf{u}}_{g_{1:i}}\right)}{\partial \boldsymbol{\theta}} - \left(\boldsymbol{\theta} - \hat{\boldsymbol{\theta}}_i^-\right)^T \left(\hat{\mathbf{P}}_i^-\right)^{-1} = \mathbf{0} \tag{13}$$

in which $\hat{\boldsymbol{\theta}}_i^-$ and $\hat{\mathbf{P}}_i^-$ are the prior estimates of the mean and covariance matrix of $\boldsymbol{\Theta}$ at time step *i*, respectively. Eq. (13) is a nonlinear algebraic equation, which can be solved approximately using a first-order approximation

of the nonlinear function $\mathbf{h}_i(\boldsymbol{\theta}, \ddot{\mathbf{u}}_{g_{1:i}})$ which represents the nonlinear finite element response function. The first-order Taylor series expansion of $\mathbf{h}_i(\boldsymbol{\theta}, \ddot{\mathbf{u}}_{g_{1:i}})$ at $\hat{\boldsymbol{\theta}}_i^-$ can be expressed as

$$\mathbf{h}_i(\boldsymbol{\theta}, \ddot{\mathbf{u}}_{g_{1:i}}) \cong \mathbf{h}_i(\hat{\boldsymbol{\theta}}_i^-, \ddot{\mathbf{u}}_{g_{1:i}}) + \mathbf{C}_i(\boldsymbol{\theta} - \hat{\boldsymbol{\theta}}_i^-) \tag{14}$$

where $\mathbf{C}_i = \left[\partial \mathbf{h}_i\left(\boldsymbol{\theta}, \ddot{\mathbf{u}}_{g_{1:i}}\right) \Big/ \partial \boldsymbol{\theta}\right]\Big|_{\hat{\boldsymbol{\theta}}_i^-}$ = FE response sensitivity matrix computed at $\boldsymbol{\theta} = \hat{\boldsymbol{\theta}}_i^-$. Substitution of Eq. (14) into Eq. (13) results in the following posterior mean estimate of $\boldsymbol{\Theta}$ at time step *i*:

$$\hat{\boldsymbol{\theta}}_i^+ = \hat{\boldsymbol{\theta}}_i^- + [\mathbf{C}_i^T \mathbf{R}^{-1} \mathbf{C}_i + (\hat{\mathbf{P}}_i^-)^{-1}]^{-1} \mathbf{C}_i^T \mathbf{R}^{-1} [\mathbf{y}_i - \mathbf{h}_i(\hat{\boldsymbol{\theta}}_i^-, \ddot{\mathbf{u}}_{g_{1:i}})] \tag{15}$$

in which $[\mathbf{C}_i^T \mathbf{R}^{-1} \mathbf{C}_i + (\hat{\mathbf{P}}_i^-)^{-1}]^{-1} \mathbf{C}_i^T \mathbf{R}^{-1} = \mathbf{K}_i$ is known as the Kalman gain matrix. It can be shown that the Kalman gain matrix can also be expressed as

$$\mathbf{K}_i = \mathbf{P}_i^{\boldsymbol{\theta}\mathbf{y}} (\mathbf{P}_i^{\mathbf{yy}})^{-1} \tag{16}$$

where $\mathbf{P}_i^{\boldsymbol{\theta}\mathbf{y}} = \hat{\mathbf{P}}_i^- \mathbf{C}_i^T$ = cross-covariance matrix of $\boldsymbol{\Theta}$ and $\mathbf{Y}$ at time step *i* and $\mathbf{P}_i^{\mathbf{yy}} = \mathbf{C}_i \hat{\mathbf{P}}_i^- \mathbf{C}_i^T + \mathbf{R}$ = covariance matrix of $\mathbf{Y}$ at time step *i*. Therefore, the posterior mean estimate of $\boldsymbol{\Theta}$ at time step *i* can be found as

$$\hat{\boldsymbol{\theta}}_i^+ = \hat{\boldsymbol{\theta}}_i^- + \mathbf{K}_i [\mathbf{y}_i - \mathbf{h}_i(\hat{\boldsymbol{\theta}}_i^-, \ddot{\mathbf{u}}_{g_{1:i}})] \tag{17}$$

The posterior covariance matrix of $\boldsymbol{\Theta}$ can be approximated using the PCRLB theorem and the matrix inversion lemma as

$$\hat{\mathbf{P}}_i^+ = (\mathbf{I} - \mathbf{K}_i \mathbf{C}_i)\, \hat{\mathbf{P}}_i^- = \hat{\mathbf{P}}_i^- - \mathbf{K}_i \mathbf{P}_i^{\mathbf{yy}} \mathbf{K}_i^T \tag{18}$$

Therefore, at each time step, the prior estimates of the mean and covariance matrix of the parameter vector $\boldsymbol{\Theta}$ are updated to the posterior estimates based on the observed discrepancies between the measured and estimated responses. The posterior estimates of the mean and covariance matrix of $\boldsymbol{\Theta}$ are then transferred to prior estimates at the next time step and the estimation process continues in time. However, to improve the convergence of the recursive estimation procedure, a random disturbance referred to as process noise is added to the estimation process. This process noise ($\boldsymbol{\gamma}$) is modeled as a stationary independent zero mean Gaussian white noise random vector with a time-invariant diagonal covariance matrix **Q**. Thus, at each time step, **Q** is added to the posterior covariance matrix of $\boldsymbol{\Theta}$ to yield the prior covariance matrix of $\boldsymbol{\Theta}$ at the next time step, i.e.,

$$\boldsymbol{\Theta}_{i+1}^- = \boldsymbol{\Theta}_i^+ + \boldsymbol{\gamma} \Rightarrow \hat{\boldsymbol{\theta}}_{i+1}^- = \hat{\boldsymbol{\theta}}_i^+,\ \hat{\mathbf{P}}_{i+1}^- = \hat{\mathbf{P}}_i^+ + \mathbf{Q} \tag{19}$$

This recursive MAP estimation procedure using linearization (with respect to $\boldsymbol{\theta}$) of the nonlinear FE model is referred to as the EKF method. By the linearization of the nonlinear FE model, the likelihood function shown in Eq. (6) will be a Gaussian function of $\boldsymbol{\theta}$. Assuming a Gaussian prior joint PDF of the FE model parameters $\boldsymbol{\Theta}$, the posterior joint PDF will also be Gaussian (see Eq. (5)). Therefore, the MAP estimate is the mean of the posterior joint PDF of $\boldsymbol{\Theta}$.

2.2.2 Unscented Kalman filter (UKF)

The UKF is similar to the EKF but it uses the unscented transformation (UT) [15], a deterministic sampling approach, to propagate the uncertainty in $\boldsymbol{\Theta}$ through the nonlinear FE model (see Eq. (2)), thus circumventing the linearization of the FE model used in the EKF method (Eq. (14)). Therefore, it results in a more accurate estimation of the posterior mean and covariance matrix of the parameter vector $\boldsymbol{\Theta}$, especially for highly nonlinear (FE) models (with respect to $\boldsymbol{\theta}$). The UT provides a more accurate estimation of $\mathbf{P}^{\boldsymbol{\theta}\mathbf{y}}$ and $\mathbf{P}^{\mathbf{yy}}$ and, therefore, of the Kalman gain matrix (see Eq. (16)).

The UKF evaluates the nonlinear FE model at a set of deterministically selected realizations of the FE model parameter vector $\boldsymbol{\Theta}$, referred to as sigma points (SPs) and denoted by $\boldsymbol{\vartheta}_i^{-,j}$, taken around the prior mean estimate $\hat{\boldsymbol{\theta}}_i^-$. In this study, a scaled UT is selected and, therefore, the number of SPs is $(2n_{\boldsymbol{\theta}} + 1)$, i.e., $j = 1, ..., 2n_{\boldsymbol{\theta}} + 1$. The weighted sample mean and covariance matrix of the SPs are equal to the prior mean estimate ($\hat{\boldsymbol{\theta}}_i^-$) and prior covariance matrix estimate ($\hat{\mathbf{P}}_i^-$) of the parameter vector $\boldsymbol{\theta}$, respectively. The SPs are propagated through the nonlinear FE model yielding

$$\mathbf{y}_i^j = \mathbf{h}_i\left(\vartheta_i^{-,j}, \ddot{\mathbf{u}}_{g_{1:i}}\right) \tag{20}$$

The mean and covariance matrix of the FE predicted structural response $\mathbf{Y}$, and the cross-covariance matrix of $\boldsymbol{\Theta}$ and $\mathbf{Y}$ are respectively computed as [7]

$$\mathbf{h}_i\left(\boldsymbol{\theta}, \ddot{\mathbf{u}}_{g_{1:i}}\right) = \sum_{j=1}^{2n_\theta+1} W_m^j \mathbf{y}_i^j \qquad \mathbf{P}_i^{yy} = \sum_{j=1}^{2n_\theta+1} W_c^j \left[\mathbf{y}_i^j - \mathbf{h}_i\left(\boldsymbol{\theta}, \ddot{\mathbf{u}}_{g_{1:i}}\right)\right]\left[\mathbf{y}_i^j - \mathbf{h}_i\left(\boldsymbol{\theta}, \ddot{\mathbf{u}}_{g_{1:i}}\right)\right]^T + \mathbf{R}$$
$$\mathbf{P}_i^{\theta y} = \sum_{j=1}^{2n_\theta+1} W_c^j \left[\vartheta_i^{-,j} - \hat{\boldsymbol{\theta}}_i^-\right]\left[\mathbf{y}_i^j - \mathbf{h}_i\left(\boldsymbol{\theta}, \ddot{\mathbf{u}}_{g_{1:i}}\right)\right]^T \tag{21}$$

where W_m^j and W_c^j denote the mean and covariance weighting coefficients, respectively. The Kalman gain matrix, posterior mean and covariance matrix estimates of $\boldsymbol{\theta}$ at time step i are obtained from Eqs. (16), (17), and (18), respectively.

3. Application example

Simulated dynamic response data from a 3D five-story two-by-one bay RC frame building subjected to bi-directional horizontal seismic excitation are used to verify the FE model updating methodologies. A mechanics-based nonlinear FE model of the building, developed in OpenSees [16], is used for response simulation. The simulated response data are contaminated with additive zero-mean white Gaussian noise and used as measured data to estimate the parameters characterizing the nonlinear material models of concrete and reinforcing steel.

The structure is designed according to the 2012 International Building Code [17] as an intermediate moment-resisting RC frame located in downtown Seattle, Washington, with Site Class D soil conditions, a short-period spectral acceleration $S_{MS} = 1.37g$, and a one-second spectral acceleration $S_{M1} = 0.53g$. The building has two bays in the longitudinal direction (X) and one bay in the transverse direction (Z), with plan dimensions of 10.0×6.0 m, respectively. The frame has five stories with a floor-to-floor height of 4.0 m. Grade 75 and Grade 60 reinforcing steel is assumed for the columns and beams, respectively. Fig. 1a shows the overall geometry of the building, the cross-sections of the beams and columns, and details of the reinforcement of the elements.

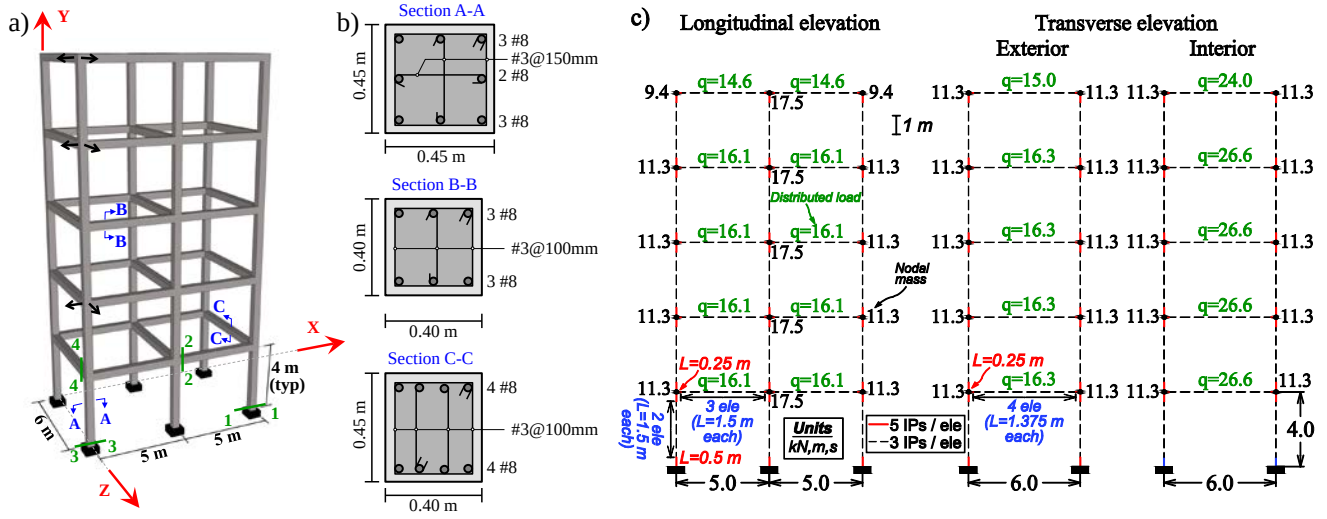

Fig. 1 – RC frame building: (a) Isometric view (black arrows indicate the locations and directions of the measured acceleration responses), (b) Cross-sections of beams and columns, (c) Finite element model.

Fig. 1b shows the FE model details for the RC frame building. Nonlinear fiber-section displacement-based frame elements [18] are used to model the beams and columns and Gauss-Lobatto quadrature is used for numerical integration along the elements. The stress-strain behavior of the fibers is governed by nonlinear uniaxial material constitutive laws. Material constitutive models depend on a set of parameters, the estimation of which is the objective of the nonlinear FE model updating approaches presented in this paper. The cross-sections

of beams and columns are discretized into longitudinal fibers as illustrated in Fig. 2a. Linear force-deformation models for shear and torsion are defined (aggregated) at the section level and along the element, but the shear is coupled with bending only at the element level through equilibrium.

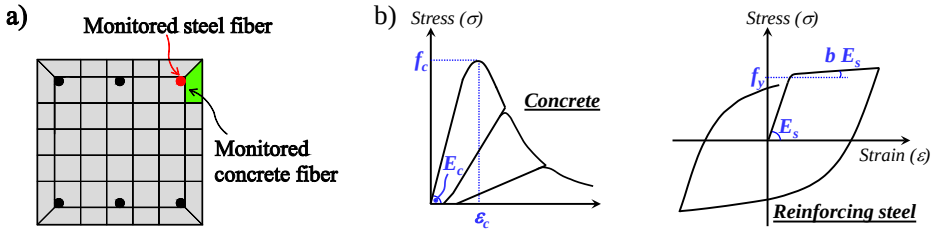

Fig. 2 – (a) Cross-section fiber discretization, (b) uniaxial material models for concrete and reinforcing steel.

The modified Giuffré-Menegotto-Pinto model [19] is used to model the nonlinear uniaxial stress-strain behavior of the longitudinal steel reinforcing bars. The primary material parameters consist of the elastic modulus (E_s), initial yield strength (f_y), and strain hardening ratio (b) and they are considered unknown parameters and estimated using the FE model updating methodologies. The Popovics-Saenz model [20],[21], which is characterized by five material parameters, is used to model the nonlinear uniaxial stress-strain behavior of the concrete fibers. The concrete material model parameters are the modulus of elasticity (E_c), peak compressive strength (f_c), strain at peak compressive strength (ε_c), crushing strength (f_u), and strain at crushing strength (ε_u). The values of f_c, ε_c, f_u, and ε_u correspond to the confined state of concrete and for response simulation purposes are determined based on the initial properties of the concrete material. The confinement effects of the transverse reinforcement on the concrete compressive strength and ductility are accounted for by modifying the parameters f_c and ε_c according to Mander et al. [22] and ε_u as suggested by Scott et al. [23]. Fig. 2b shows the uniaxial material constitutive models used for the concrete and reinforcing steel fibers with their corresponding parameters assumed to be unknown in the estimation phase. A set of material parameter values, referred to as true values, are assumed for the concrete and reinforcing steel materials in order to simulate the response of the structure. These parameter values are: $E_{s-col}^{true} = 200\,\text{GPa}$, $f_{y-col}^{true} = 517\,\text{MPa}$, $b_{col}^{true} = 0.01$, $E_{s-beam}^{true} = 200\,\text{GPa}$, $f_{y-beam}^{true} = 414\,\text{MPa}$, $b_{beam}^{true} = 0.05$, $E_c^{true} = 27600\,\text{MPa}$, $f_c^{true} = 40\,\text{MPa}$, and $\varepsilon_c^{true} = 0.0035$. The concrete parameters f_u and ε_u are not considered as estimation parameters, since in this case study they have negligible effects on the response of the structure. The damping energy dissipation (beyond the energy dissipated through hysteretic material behavior) are modeled using mass and tangent stiffness-proportional Rayleigh damping. A critical damping ratio of 2% for the first and second modes (T_1 = 2.01 sec and T_2 = 0.64 sec, after application of gravity) is considered. Consequently, the mass and stiffness proportional parameters used to describe the Rayleigh damping are $\alpha_M = 0.0948$ and $\beta_K = 0.0031$, respectively. The horizontal components of the ground acceleration recorded at the Sylmar County Hospital during the 1994 Northridge earthquake (Fig. 3) are used as input base excitation ($\ddot{\mathbf{u}}_g$). The 360° and 90° components are applied in the longitudinal and transverse direction of the building, respectively.

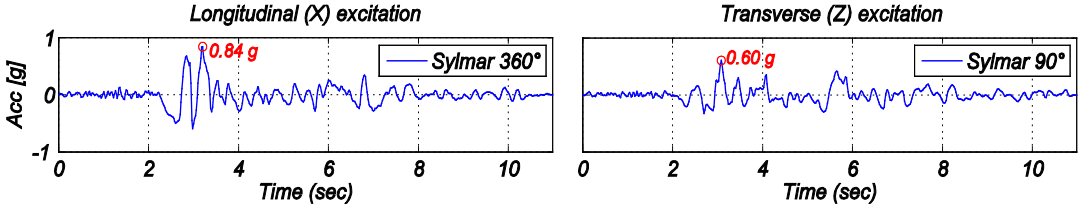

Fig. 3 – Ground acceleration records used as seismic input motions.

3.1 Bayesian FE model updating

The nonlinear FE model presented above with the true material parameter values ($\boldsymbol{\theta}^{true} = [E_{s-col}^{true}, f_{y-col}^{true}, b_{col}^{true}, E_{s-beam}^{true}, f_{y-beam}^{true}, b_{beam}^{true}, E_c^{true}, f_c^{true}, \varepsilon_c^{true}]^T \in \mathbb{R}^{9\times 1}$) is subjected to the earthquake input motion

shown in Fig. 3 and used to define the true response of the structure. After completion of the response simulation, the true relative horizontal acceleration responses at the 3rd, 5th, and roof levels in both the longitudinal (X) and transverse (Z) directions (see black arrows in Fig. 1) are contaminated with 1.0%*g* root-mean-square (RMS) additive zero-mean Gaussian white noise and used as measured output ($\mathbf{y}$) in the estimation phase. The true covariance matrix of the output measurement noise is $(0.01g)^2\mathbf{I}_6 = 0.96\times10^{-2}\mathbf{I}_6(m/s^2)^2$ where $\mathbf{I}_j$ = j × j identity matrix. Statistically independent realizations of output measurement noise are used for different responses. It is noted that a noise level of 1.0%g RMS is considerably larger than the level of noise expected from accelerometers currently used in earthquake engineering. Nevertheless, this relatively high level of measurement noise is considered to examine the performance and robustness of the proposed parameter estimation process under extremely noisy conditions. It is assumed that the noiseless seismic input is available in the parameter estimation phase. The batch and recursive Bayesian estimation approaches presented in Section 2 are used to estimate the unknown FE model parameters ($\boldsymbol{\theta} = [E_{s-col}, f_{y-col}, b_{col}, E_{s-beam}, f_{y-beam}, b_{beam}, E_c, f_c, \varepsilon_c]^T$) and to update the nonlinear FE model of the structure. The initial estimates of the expected values of the model parameters ($\hat{\boldsymbol{\theta}}_0$) are taken as $\hat{\boldsymbol{\theta}}_0 / \boldsymbol{\theta}^{true} = [0.70, 1.30, 1.25, 1.30, 0.80, 0.75, 1.20, 0.85, 0.90]^T$.

For the recursive approaches (UKF and EKF), it is assumed that the output measurement noise is a zero-mean white Gaussian process with a covariance matrix $\mathbf{R} = 0.47\times10^{-2}\mathbf{I}_6(m/s^2)^2$, i.e., a standard deviation (or RMS) of 0.7%*g*. The assumed amplitude of the measurement noise is purposely chosen to be different from the true amplitude, since in a real-world application the exact measurement noise amplitude is unknown and should be estimated based on the characteristics of the sensors and DAQ system used, experience, and engineering judgment. Time-invariant first- and second-order statistics are assumed for the process noise, with zero-mean and covariance matrix $\mathbf{Q}_k = \mathbf{Q}$. The diagonal entries of $\mathbf{Q}$ are taken as $(q\times\hat{\theta}_{0_n})^2$ where $n = 1,...,9$ and $q = 1\times10^{-5}$. The initial estimate of the covariance matrix of the model parameters, $\hat{\mathbf{P}}_0$, is assumed to be diagonal (i.e., initial estimates of the FE model parameters are assumed statistically uncorrelated). Diagonal entries of $\hat{\mathbf{P}}_0$ are taken as $(p\times\hat{\theta}_{0_n})^2$ where $n = 1,...,9$ and $p = 0.15$.

Two cases are considered in the batch Bayesian estimation approach. In the first case, $\boldsymbol{\theta}$ and the diagonal entries of the measurement noise variance matrix ($\mathbf{r} \in \mathbb{R}^{6\times1}$) are jointly estimated though an extended optimization process as shown in Eq. (9). The initial estimate of the measurement noise variances is taken as $\hat{\mathbf{r}}_0 = 0.47\times10^{-2}[1,1,1,1,1,1]^T$ (m/ s^2)^2, corresponding to a 0.7%*g* RMS measurement noise. The feasible search domain for the model parameters and for the measurement noise variance are chosen as $0.4\hat{\boldsymbol{\theta}}_0 \le \boldsymbol{\theta} \le 2.5\hat{\boldsymbol{\theta}}_0$ and $0.01\hat{\mathbf{r}}_0 \le \mathbf{r} \le 100\hat{\mathbf{r}}_0$, respectively. In the second case, only $\boldsymbol{\theta}$ is estimated, while $\mathbf{r}$ is initially estimated (by the same value assumed for the recursive approaches for comparison purposes) and kept constant during the FE model parameter estimation process. In both cases, the parameter estimation uncertainty is quantified by evaluating the CRLB using the two methods presented in Section 2. The optimization process is considered converged when at least one of the following conditions is satisfied:

$$\text{Condition 1: } \left\| \begin{bmatrix} \hat{\bar{\boldsymbol{\theta}}}_m \\ \hat{\mathbf{r}}_m \end{bmatrix} - \begin{bmatrix} \hat{\bar{\boldsymbol{\theta}}}_{m-1} \\ \hat{\mathbf{r}}_{m-1} \end{bmatrix} \right\|_2 \le 10^{-7} \qquad \text{Condition 2: } \left\| \nabla J(\boldsymbol{\theta}, \mathbf{r}) \right\|_\infty \le 10^{-7} \tag{22}$$

where $\hat{\bar{\boldsymbol{\theta}}}_m$ = estimated normalized (with respect to the initial parameter estimates) FE model parameter vector at the m^{th} optimization iteration, $\|...\|_2$ denotes the Euclidean norm, and $\|...\|_\infty$ denotes the infinity norm. It is noted that for the second case study where the vector $\mathbf{r}$ is fixed, only $\boldsymbol{\theta}$ remain in Conditions 1 and 2.

3.1.1 Discussion of parameter estimation results

Table 1 reports the estimated FE model parameters normalized by the corresponding true values ($\hat{\theta}_n / \theta_n^{true}$) with $n = 1,...,9$ and Table 2 their corresponding coefficient of variations (C.O.V.) defined as $\hat{\sigma}_{\theta_n} / \hat{\theta}_n$, where $\hat{\sigma}_{\theta_n}$ is

the estimated standard deviation of the FE model parameter θ_n. For the recursive approaches, these quantities correspond to the estimation results obtained at the last time step, while for the batch approach, they are the converged values obtained after the convergence criteria presented in Eq. (22) are satisfied.

Table 1 – FE model parameter estimates.

Estimation method	FE Model parameter estimates ($\hat{\theta}_n / \theta_n^{true}$), $n = 1,...,9$								
	$\frac{E_{s-col}}{E_{s-col}^{true}}$	$\frac{f_{y-col}}{f_{y-col}^{true}}$	$\frac{b_{col}}{b_{col}^{true}}$	$\frac{E_{s-beam}}{E_{s-beam}^{true}}$	$\frac{f_{y-beam}}{f_{y-beam}^{true}}$	$\frac{b_{beam}}{b_{beam}^{true}}$	$\frac{E_c}{E_c^{true}}$	$\frac{f_c}{f_c^{true}}$	$\frac{\varepsilon_c}{\varepsilon_c^{true}}$
UKF	1.00	1.00	1.01	1.00	1.00	0.99	1.00	1.01	0.98
EKF	1.00	1.00	1.04	1.00	1.00	0.99	1.00	1.00	0.99
Batch with noise variance estimation	1.00	1.00	1.01	1.00	1.00	1.00	1.00	0.99	0.98
Batch without noise variance estimation	1.00	1.00	1.02	1.00	1.00	1.00	1.00	1.00	0.98

Table 2 – Parameter estimation uncertainty.

Estimation method		C.O.V. (%) of FE model parameter ($\hat{\sigma}_{\theta_n} / \hat{\theta}_n$)								
		E_{s-col}	f_{y-col}	b_{col}	E_{s-beam}	f_{y-beam}	b_{beam}	E_c	f_c	ε_c
UKF	–	0.09	0.06	1.47	0.13	0.08	0.32	0.21	0.87	1.88
EKF	–	0.11	0.07	1.58	0.15	0.09	0.31	0.33	0.95	2.11
Batch with noise var. estimation	Method 1	0.15	0.10	2.27	0.21	0.13	0.43	0.50	1.29	3.03
	Method 2	0.16	0.11	2.45	0.25	0.13	0.33	0.55	1.33	3.45
Batch without noise var. estimation	Method 1	0.11	0.07	1.59	0.15	0.09	0.31	0.35	0.91	2.12
	Method 2	0.11	0.07	1.62	0.15	0.10	0.30	0.32	0.84	2.13

Excellent results are obtained with the different estimation methods, with relative estimation errors less than or equal to 4% for all nine FE model parameters. Material initial stiffness (E_{s-col}, E_{s-beam}, and E_c) and yield parameters of reinforcing steel (f_{y-col} and f_{y-beam}) are accurately estimated using all the estimation methods. Material model parameters b_{col}, b_{beam}, f_c, and ε_c are estimated with larger relative errors ($\leq$ 4%) and they are associated with larger estimation uncertainty as can be inferred from their C.O.V.s that are ranging between 0.3 and 3.5%. Since the measured output responses are less sensitive to b_{col} and ε_c, i.e., less information about these parameters is contained in $\mathbf{y}$, larger relative errors and C.O.V.s in their final estimates are observed.

Fig. 4 show the convergence history of the nine FE model parameters using the recursive and batch estimation approaches. In the recursive approach, the initial-stiffness related material parameters (E_{s-col}, E_{s-beam}, and E_c) start updating from the first time steps because the output responses are sensitive to elastic-related material parameters at all levels of excitation. These parameters converge to their true values at about the 4th second of excitation. It should be noted that the FE acceleration response sensitivities with respect to E_c are much higher than those to other material parameters during the first two seconds. Since the EKF is based on the analytical linearization of the nonlinear FE response, a large and abrupt jump in the recursive estimate of E_c is observed at the beginning of the excitation. The UKF shows a smoother convergence because this approach circumvents the analytical differentiation of the nonlinear FE response prediction with respect to the estimation parameters. In addition, in the UKF, a parameter controlling the spread of the SPs around the mean value (set equal to 0.01 in this study) allows to control the rate of convergence of the filter (see [7] for more details). The other material model parameters start updating at about or after the 2nd second of the excitation, when the amplitude of the excitation increases abruptly (see Fig. 3). The yield strength of the reinforcing steel (f_{y-col} and f_{y-beam}), the strain hardening ratio of the reinforcing steel in the beams (b_{beam}), and the compressive

strength of the concrete (f_c) quickly converge to their true values. Estimates of the strain hardening ratio of the column reinforcing steel (b_{col}) and of the strain at the peak compressive strength of concrete (ε_c) are moving towards and approaching their true values. However, these estimates do not fully stabilize and fluctuate until the end of the time history, because there is not enough information about these two parameters in the output measured response. In the case of the batch estimation approach (Fig. 4b), the number of iterations corresponds to the number of evaluations of the objective function defined in Eq. (10). As explained in [10], the spike-like behavior in the convergence histories of the estimated model parameters is due to perturbations applied by the optimization algorithm to escape from the attraction zones of local minima. Both batch estimation solutions (marked by dots in Fig. 4b) converge to the true values of the parameters; however, a large number of iterations is required for the extended estimation process, when $\mathbf{r}$ and the FE model parameters $\boldsymbol{\theta}$ are estimated jointly.

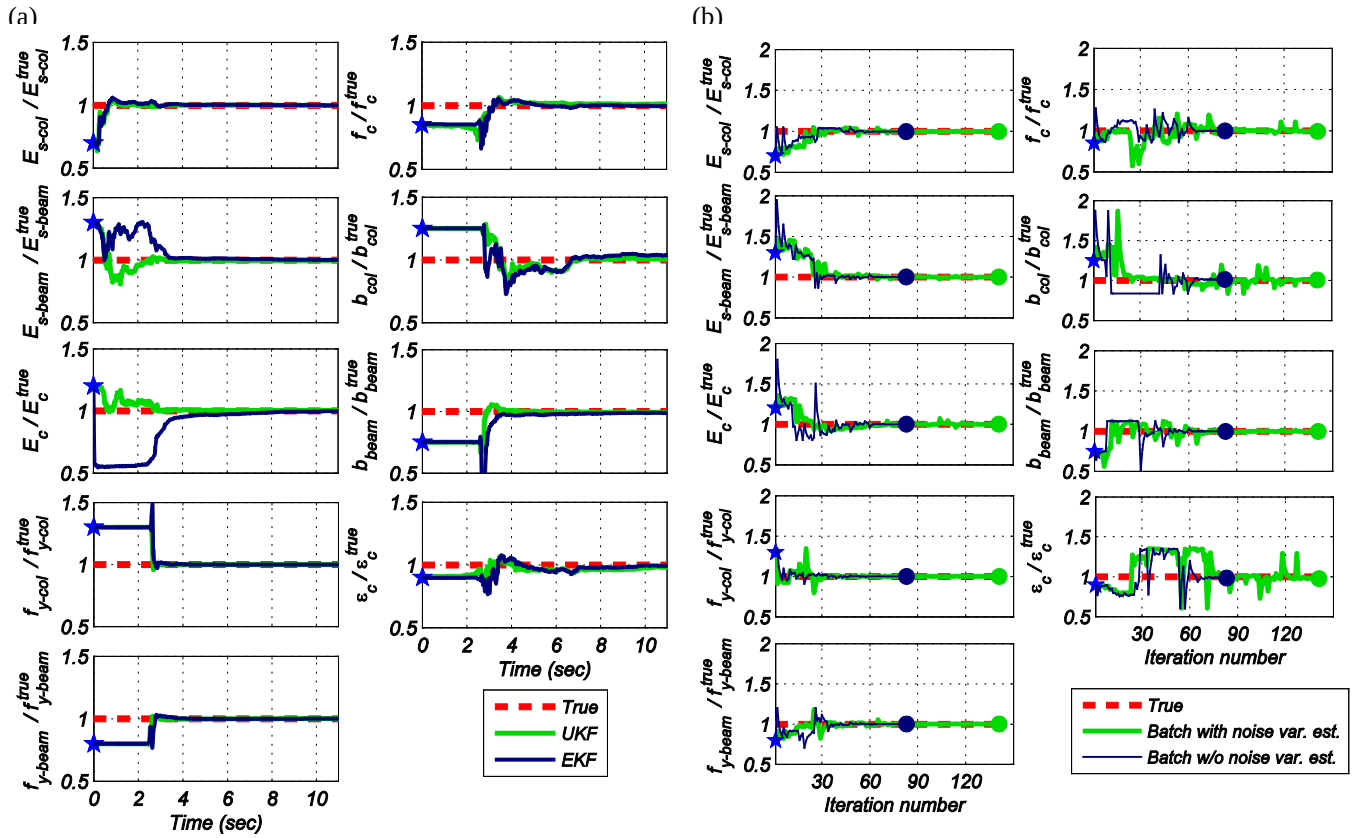

Fig. 4 – Posterior estimates of the FE model parameters: (a) recursive approach, (b) bath approach.

The updated FE model can be used to reconstruct unobserved (unmeasured) responses quantities at global and local levels that can be used to define and quantify damage indices from which the degree of damage throughout the structure can be assessed. Such damage indices include those based on maximum inelastic deformation responses at different scales (e.g., maximum displacement or curvature or strain ductility factors) or normalized cumulative hysteretic energy dissipated (e.g., cumulative displacement, curvature or strain ductility) as a measure of cumulative damage (e.g., low-cycle fatigue), or a combination of both. Fig. 5 compares different force-deformation response histories at different scales (structure, section and fiber levels) computed with the true FE model parameters and with the final estimates of the model parameters obtained using the UKF and batch (without noise variance estimation) approaches. The total base shear in the longitudinal and transverse directions (V_b^x and V_b^z, respectively) normalized by the total weight of the building (W) versus the roof drift ratio in the corresponding direction (RDR^x and RDR^z) are plotted in Fig. 5a–b, respectively. The moment (M) versus curvature (κ) for sections at the base of a column (section 1–1 in Fig. 1a) and at the end of a 2nd floor longitudinal beam (section 2–2 in Fig. 1a) are shown in Fig. 5c–d, respectively. Fiber level responses are presented in Fig. 5e–f, where the stress (σ) versus strain (ε) of a monitored reinforcing steel fiber at the bottom

of a column (section 3−3 in Fig. 1a) and a monitored concrete fiber at the end of a 2nd floor transverse beam (section 4−4 in Fig. 1a) are plotted. The excellent agreement between the true and estimated response based on the final estimates of the model parameters corroborates that the updated FE models can be reliably used for damage identification purposes.

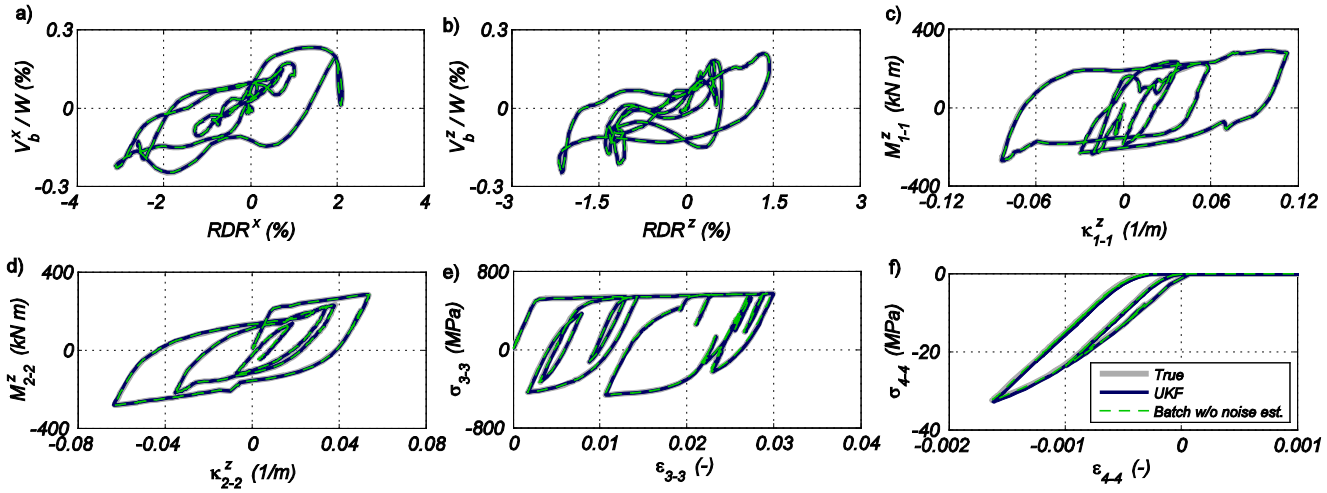

Fig. 5 – Comparison of unobserved FE responses computed with the true FE model parameters and final estimates of the FE model parameters obtained using the UKF and batch estimation approaches: (a) V_b^x vs. RDR^x, (b) V_b^z vs. RDR^z, (c) M vs. κ at the base of a column (section 1−1 in Fig. 1a), (d) M vs. κ at the end of a longitudinal beam (section 2−2 in Fig. 1a), (e) σ vs. ε of a reinforcing steel fiber at the bottom of a column (section 3−3 in Fig. 1a), (f) σ vs. ε of a concrete fiber at the end of a transverse beam (section 4−4 in Fig. 1a).

4. Conclusions

This study investigated and compared the performance of a new framework to identify and update mechanics-based nonlinear structural finite element (FE) models using different Bayesian estimation methods. The framework uses recorded input-output data to estimate unknown parameters of advanced mechanics-based nonlinear FE models of the structure of interest, using both batch and recursive approaches. The batch estimation approach consisted of the maximum a posteriori method, which results in a nonlinear optimization problem that is solved using the interior point method, a gradient-based optimization algorithm. The Extended Kalman filter and Unscented Kalman filter were employed as recursive Bayesian estimation methods. The proposed methodology was verified using numerically simulated structural response data for a three-dimensional five-story two-by-one bay reinforced concrete frame building subjected to bi-directional horizontal earthquake excitation. Parameters characterizing the nonlinear material constitutive laws of the reinforcing steel and concrete materials were successfully estimated using the noiseless seismic input data together with limited noisy output response data (6 relative acceleration response time histories). Excellent results were obtained with both batch and recursive estimation methods. Comparison of unobserved response quantities at different scales (structure, component, section and fiber levels) obtained from the updated FE model and the corresponding "true" responses demonstrated the capabilities of the proposed framework for (nonlinear) damage identification purposes. Thus, the updated FE model can be used to reconstruct unmeasured structural responses from the global to local levels. The reconstructed inelastic structural response can be utilized to estimate mechanics-based damage indices and therefore to assess the type and level of damage throughout the structure.

5. References

[1] E. Simoen, G. De Roeck, and G. Lombaert. (2015). "Dealing with uncertainty in model updating for damage assessment: A review." Mechanical Systems and Signal Processing, 56-57, 123–149.

[2] J. Ching, J.L. Beck, K.A. Porter, and R. Shaikhutdinov. (2006). "Bayesian state estimation method for nonlinear systems and its application to recorded seismic response." ASCE Journal of Engineering Mechanics, 132(4), 396–410.

[3] J. Yang, Y. Xia, and C.H. Loh. (2014). "Damage detection of hysteretic structures with pinching effect." ASCE Journal of Engineering Mechanics, 140(3), 462–472.

[4] N. Distefano and A. Rath. (1975). "System identification in nonlinear structural seismic dynamics." Computer methods in applied mechanics and engineering, 5, 353–372.

[5] N. Distefano and B. Pena-Pardo. (1976). "System identification of frames under seismic loads." Journal of the Engineering Mechanics, Division, 102(EM2), 313–330.

[6] S. Shahidi and S. Pakzad. (2014). "Generalized response surface model updating using time domain data." ASCE Journal of Structural Engineering, 140, Special Issue: Computational Simulation in Structural Engineering, A4014001.

[7] R. Astroza, E. Ebrahimian, and J.P. Conte. (2015). "Material parameter identification in distributed plasticity FE models of frame-type structures using nonlinear stochastic filtering." ASCE Journal of Engineering Mechanics, 141(5), 04014149.

[8] H. Ebrahimian, R. Astroza, and J.P. Conte. (2015). "Extended Kalman filter for material parameter estimation in nonlinear structural finite element models using direct differentiation method." Earthquake Engineering & Structural Dynamics, 44(10), 1495–1522.

[9] J.J. Tsay and J.S. Arora. (1990). "Nonlinear structural design sensitivity analysis for path dependent problems. Part 1: General theory." Computer Methods in Applied Mechanics and Engineering, 81(2), 183–208.

[10] H. Ebrahimian, R. Astroza, J.P. Conte, and R.A. de Callafon. (2016). "Nonlinear finite element model updating for damage identification of civil structures using batch Bayesian estimation." Mechanical Systems and Signal Processing, Special Issue on Nonlinear System Identification, Accepted for publication.

[11] R.H. Byrd, M.E. Hribar, and J. Nocedal. (1999). "An interior point algorithm for large-scale nonlinear programming." SIAM Journal on Optimization, 9(4), 877–900.

[12] M. Kleiber, H. Antunez, T.D. Hien, and P. Kowalczyk. (1997). Parameter sensitivity in nonlinear mechanics: Theory and finite element computations. John Wiley and Sons, England.

[13] H.L. Van Trees. (2002). Optimum array processing, Part IV of detection, estimation, and modulation theory. New York, NY: John Wiley & Sons.

[14] P.E. Gill, W. Murray, and M.H. Wright. (1981). Practical optimization. Academic Press, London, England.

[15] S.J. Julier and J.K. Uhlmann. (1997). "A new extension of the Kalman filter to nonlinear systems." 11th International Symposium on Aerospace/Defense Sensing, Simulation and Controls, Orlando, FL.

[16] OpenSees. Open System for Earthquake Engineering Simulation. [Online]. Available: http://opensees.berkeley.edu.

[17] International Code Council (ICC). (2012). International Building Code. Falls Church, VA.

[18] F.F. Taucer, E. Spacone, and F.C. Filippou. (1991). A fiber beam-column element for seismic response analysis of reinforced concrete structures. Report 91/17, EERC, Earthquake Engineering Research Center (EERC), University of California, Berkeley.

[19] F.C. Filippou, E.P. Popov, and V.V. Bertero. (1983). Effects of bond deterioration on hysteretic behavior of reinforced concrete joints. UCB/EERC-83/19, Berkeley, CA: EERC Report 83-19, Earthquake Engineering Research Center.

[20] S. Popovics. (1973). "A numerical approach to the complete stress–strain curve of concrete." Cement Concrete Research, 3(5), 583–599.

[21] T.A. Balan, E. Spacone, and M. Kwon. (2001). "A 3D hypoplastic model for cyclic analysis of concrete structures." Engineering Structures, 23(4), 333–342.

[22] J.B. Mander, M.J.N. Priestley, and R. Park. (1988). "Theoretical stress-strain model for confined concrete." ASCE Journal of Structural Engineering, 114(8), 1804–1826.

[23] B.D. Scott, R. Park, and M.J.N. Priestley. (1982). "Stress-strain behavior of concrete confined by overlapping hoops at low and high strain rates." American Concrete Institute (ACI) Journal, 79(1), 13–27.